J Mater Sci (2008) 43:5092–5101
DOI 10.1007/s10853-008-2755-2

REVIEW

Processing of nanographene platelets (NGPs) and NGP nanocomposites: a review

B. Z. Jang · A. Zhamu

Received: 21 March 2008 / Accepted: 28 May 2008 / Published online: 24 June 2008

Abstract The *nanoscale graphene platelet* (NGP) or *graphene nanosheet* is an emerging class of nanomaterials. An NGP is a nanoscale platelet composed of one or more layers of a graphene plane, with a platelet thickness from less than 0.34 to 100 nm. NGPs are predicted to have a range of unusual physical, chemical, and mechanical properties. Although practical electronic device applications for graphene are not envisioned to occur within the next 5–10 years, its application as a nanofiller in a composite material is imminent. The availability of processable graphene sheets in large quantities is essential to the success in exploiting composite and other applications. This review first describes the earlier processes for producing mostly multi-layer NGPs and their composites, which is followed by a discussion on the recent developments in the preparation of single-layer NGPs and their nanocomposites. Fundamental principles behind processing of nanographene materials are also briefly discussed.

Introduction

For more than six decades, scientists have presumed that a single-layer graphene sheet (one atom thick) could not exist in its free state based on the reasoning that its planar structure would be thermodynamically unstable. Somewhat surprisingly, several groups worldwide have recently succeeded in obtaining isolated graphene sheets [1–9]. Several unique properties associated with these 2-D crystals have been discovered [10–18]. In addition to single graphene sheets, double-layer or multiple-layer graphene sheets also exhibit unique and useful behaviors. In the present context, single-layer and multiple-layer graphene sheet structures are collectively referred to as *nanographene platelets* (NGPs).

Carbon nanotubes (CNTs) and NGPs exhibit some similar behaviors, but some vastly distinct properties. For instance, electrons in a single-layer NGP are believed to behave like massless chiral relativistic particles [10–14], as reflected by the anomalous quantization of the Hall conductance. An NGP has an edge-inherited non-bonding π state, which could result in unconventional nanomagnetic properties, such as spin glass states, magnetic switching, and edge-state spin gas probing [15]. In a Josephson junction configuration, an NGP shows a bipolar supercurrent [16]. An NGP of a few atoms thick is found to be a two-dimensional semi-metal with a small overlap between valence and conduction bands [2]. Additionally, NGP-based nanocomposites are found to exhibit a range of unique and useful properties [19–25].

Selected physical and mechanical properties of NGPs, CNTs, and vapor-grown carbon nanofibers ([VG-CNFs], considered as the larger-diameter cousins of CNTs) are presented in Table 1.

Pre-2004 work on NGPs and NGP composites

Isolated NGPs

Earlier attempts to produce NGPs dated back to late 1980s, although the significance of NGPs was not well recognized

B. Z. Jang (✉)
College of Engineering and Computer Science, Wright State University, 3640 Colonel Glenn Hwy., Dayton, OH 45435, USA
e-mail: Bor.Jang@wright.edu

A. Zhamu
Angstron Materials, LLC, 1240 McCook Ave., Dayton, OH 45404, USA
e-mail: Aruna.Zhamu@AngstronMaterials.com

Table 1 Estimated physical constants of CNTs, CNFs, and NGPs

Property	Single-walled CNTs	Carbon nanofibers	NGPs
Specific gravity	0.8 g/cm^3	1.8 (AG)–2.1 (HT) g/cm^3 AG = as grown; HT = heat-treated (graphitic)	1.8–2.2 g/cm^3
Elastic modulus	~1 TPa (axial direction)	0.4 (AG)–0.6 (HT) TPa	~1 TPa (in-plane)
Strength	50–500 GPa	2.7 (AG)–7.0 (HT) GPa	~100–400 GPa
Resistivity	5–50 μΩ cm	55 (HT)–1000 (AG) μΩ cm	50 μΩ cm (in-plane)
Thermal conductivity	Up to 2,900 Wm^{-1} K^{-1} (estimated)	20 (AG)–1950 (HT) Wm^{-1} K^{-1}	5,300 Wm^{-1} K^{-1} (in-plane) 6–30 Wm^{-1} K^{-1} (*c*-axis)
Magnetic susceptibility	22 × 10^6 emu/g (radial) 0.5 × 10^6 emu/g (axial)	N/A	22 × 10^6 emu/g (⊥ to plane); 0.5 × 10^6 emu/g (‖ to plane)
Thermal expansion	Negligible in the axial direction	−1 × 10^{-6} K^{-1} (HT; axial)	−1 × 10^{-6} K^{-1} (in-plane) 29 × 10^{-6} K^{-1} (*c*-axis)
Thermal stability	>700 °C (in air); 2800 °C (in vacuum)	450–650 °C (in air)	450–650 °C (in air)
Specific surface area	Typically 10–200 m^2/g Up to 1,300 m^2/g	10–60 m^2/g	Typically 100–1,000 m^2/g, up to >2,600) m^2/g

These data were obtained from various open-literature sources and our own estimations

and similar materials were referred to as *thin graphite flakes* then.

Bunnell [26–28] developed a method in late 1988 that entailed intercalating graphite with a strong acid to obtain a graphite intercalation compound (GIC), thermally exfoliating the GIC to obtain discrete layers of graphite, and then subjecting the graphite layers to ultrasonic energy, mechanical shear forces, or freezing to separate the layers into discrete flakes. Technically, the acid-treated graphite was actually graphite oxide (GO), rather than pristine graphite. Although most of the flakes presented in the examples appeared to be thicker than 100 nm [28], flakes as small as 10 nm were cited. Polymer composites containing these thin flakes were also investigated by Bunnell [27, 28]. In a similar manner, Zaleski et al. [29] used air milling to further delaminate thermally exfoliated graphite flakes. The resulting structures exhibited a specific surface area of 35 m^2/g, corresponding to an average flake thickness of approximately 25 nm, based on the results of our calculations (Fig. 1). Without going through a chemical intercalation route, Mazurkiewicz [30] claimed to have produced graphite nanoplatelets having an average thickness in the range of 1–100 nm through high-pressure milling of natural flake graphite.

Shioyama [31] prepared a potassium-intercalated GIC from highly oriented pyrolytic graphite (HOPG), initiated in situ polymerization of isoprene or styrene in the intergraphene spaces, and then thermally decomposed intergraphene polymer chains at a high temperature (500–1,000 °C). The volatile gas molecules served to exfoliate graphite layers, and, after the volatile gas escaped, isolated graphene sheets were obtained. Unfortunately, Shioyama did not discuss the thickness of the isolated graphene

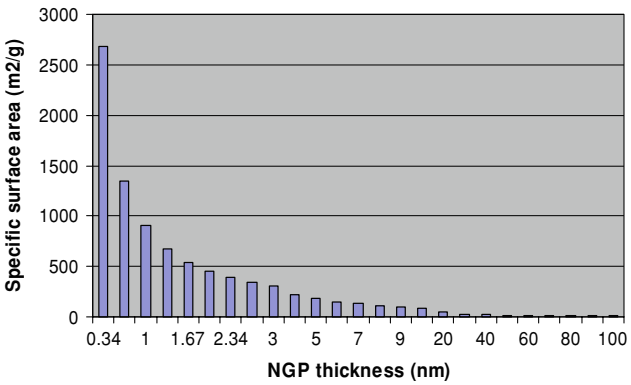

Fig. 1 Calculated specific surface areas of NGPs plotted as a function of NGP thickness (assuming NGP length and width = 5 μm)

sheets, although presumably and likely some single sheets were produced with this approach.

Jang et al. [3, 4] succeeded in isolating single-layer and multi-layer graphene structures from partially graphitized polymeric carbons, which were obtained from a polymer or pitch precursor. Shown in Fig. 2 are polymeric carbon fibers obtained by intercalating and exfoliating carbonized polyacrylonitrile (PAN) fibers. Examples of the graphene platelets extracted from these fibers using a ball milling procedure are given in Fig. 3.

Horiuchi and co-workers [32–36] have done some significant work on the preparation of nanoscaled graphite oxide (GO) platelets, which they coined as *carbon nanofilms*. These films were prepared by a two-step process—oxidation of graphite and purification of the resulting graphite oxide, with exfoliation occurring mainly in the second step. The oxidation of graphite was conducted using the now well-known Hummer's method [37, 38], which

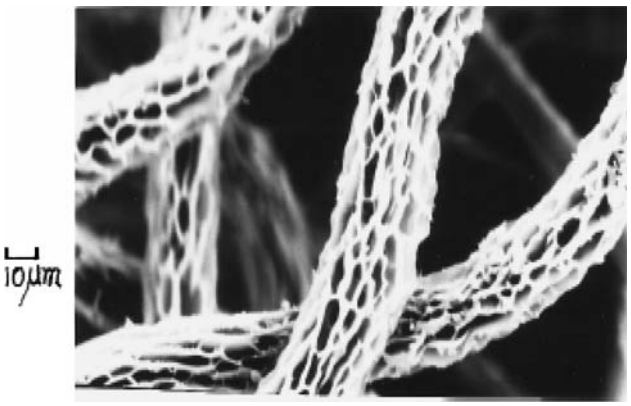

Fig. 2 A SEM image of a partially exfoliated polymeric carbon fiber

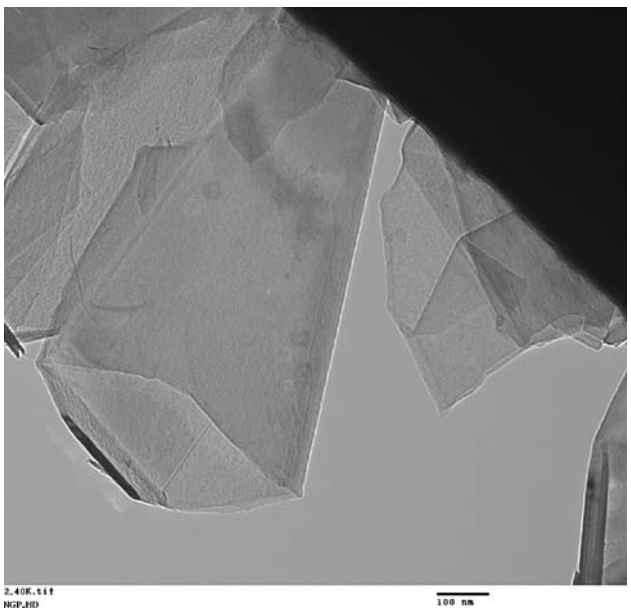

Fig. 3 TEM image of NGPs obtained from exfoliation and ball-milling of a polymeric carbon

entailed immersing natural graphite particles in a mixture of H_2SO_4, $NaNO_3$, and $KMnO_4$ to obtain graphite intercalation compounds (GICs) that actually were GOs. By hydrolyzing the GIC, functional groups, such as acidic hydroxyl groups and ether groups, were introduced into the inter-graphene layer spaces. Each of the graphite oxide layers became a multiple-charge anion, having a thickness of approximately 0.6 nm. When the excess small ions derived from the oxidants (e.g., $NaNO_3$ and $KMnO_4$) were thoroughly removed by a purification process, many layers tended to automatically separate from each other due to inter-layer electrostatic repulsion. The resulting GO layers formed a stable dispersion in water. According to Horiuchi et al. [32], single-layer graphene was detected.

It may be noted that the approach of using electrostatic repulsion to separate graphene layers was pursued in 1998 by Liu and Gong [39], as a first step in their attempt to synthesize polyaniline-intercalated GO. In a 3-D graphite crystal, the inter-layer spacing (L_d) is 0.335 nm, which is known to increase to 0.6–1.1 nm if graphite is oxidized to produce GO. Further, GO is hydrophilic and can be readily dispersed in water or aqueous solution. Dekany et al. [40] observed that the inter-graphene spacing was increased to $L_d = 1.23$ nm when GO particles were dispersed in 0.05 N NaOH solution. When dispersed in a 0.01 N NaOH solution, the spacing was essentially infinite, likely implying that GO was completely exfoliated to become a disordered structure.

A scanning probe microscope was used by Roy et al. [41] and by Lu et al. [42] to manipulate graphene layers at the step edges of graphite and etched HOPG, respectively, with the goal of fabricating ultra-thin nanostructures. It was not clear if single graphene sheets were obtained using this technique by either group. Epitaxial films of graphite with only one or a few atomic layers are of technological and scientific significance due to their peculiar characteristics and great potential as a device substrate [43–46]. This topic was reviewed by Oshima and Nagashima [47] and further discussed by Wu and Chong [48].

NGP composites

There are basically three approaches to the preparation of NGP-based composite materials. The first includes intercalation of a monomer into inter-layer spaces of GO (before and after exfoliation of GO flakes), followed by in situ polymerization. The second entails dissolution of a polymer in a solution in which graphene or GO platelets are dispersed. This category includes GO-polymer composites prepared by self-assembly. In both first and second approaches, GO may be chemically or electrochemically reduced to graphite before or after polymer addition. The third involves preparation of isolated graphene or GO platelets, which are then mixed with a polymer melt (e.g., using a twin-screw extruder).

Possibly due to the limited inter-graphene spacing (0.335 nm center-to-center, leaving behind an interstitial space of much less than 0.3 nm) and lack of functional groups on the graphene layer surfaces or at the edges, pristine graphite has not been well suited to intercalation by monomers and in situ polymerization. Thus, only a very limited amount of work [49] has been reported on the in situ polymerization in graphite. By contrast, the inter-layer spacing in GO is much larger (0.61–1.1 nm) and several functional groups (e.g., hydroxyl, carbonyl, epoxide, etc.) are often associated with GO layers, making GO an ideal material for monomer intercalation and polymerization in inter-layer spaces prior to exfoliation, or in inter-flake spaces after exfoliation.

Several polar organic compounds and polymers have been intercalated into inter-graphene or inter-flake spaces

to form intercalated or exfoliated GO nanocomposites. These include poly (vinyl alcohol) [50–52], poly (acrylamide) [53], and poly (acrylic acid) [54]. Intercalation of hydrophobic polymers, such as poly (vinyl acetate) [55], into GO was also achieved by in situ polymerization. With a thermal treatment (de-oxygenation), GO could be reduced to restore the graphene structure and its conductive properties [56]. Reduction of a polymer-GO to a polymer-graphene nanocomposite also could be accomplished electrochemically or chemically [39, 57–59]. These examples demonstrated that it was possible to prepare a polymer-GO intercalation composite as a precursor to a more conductive polymer-graphene nanocomposite.

Preparation of ultra-thin films by a layer-by-layer self-assembly approach from GO nanoplatelets and polymer electrolytes also has been investigated [60–66]. Although the original intent of these studies was primarily to fabricate self-assembled GO-poly(ethylene oxide) nanocomposites, their first step almost always involved full exfoliation and separation of GO platelets. This was evidenced by the X-ray diffraction data of the resulting structures that showed complete disappearance of those diffraction peaks corresponding to graphite oxide or pristine graphite [60, 62].

Perhaps the most heavily studied GO- or NGP-polymer nanocomposite systems have been polystyrene- (PS) and poly (methyl methacrylate)- (PMMA) based composites [67–75]. Also studied were nanocomposites based on other matrices, including nylon [76], polypropylene [77], poly (arylene disulfide) [78], and epoxy resins [22]. In most of these investigations, nanocomposites were prepared via monomer intercalation of exfoliated graphite (mostly GO), followed by polymerization. In all cases, graphite was intercalated in an acid-oxidizer mixture solution to obtain a GIC or GO sample, which was thermally exfoliated at a temperature typically in the range of 800–1,100 °C. It seemed that single-layer or double-layer graphite oxide sheets were sporadically obtained in exfoliated samples [70–72], although the researchers did not attempt to isolate these ultra-thin platelets and did not conduct a specific surface area measurement (e.g., using the well-known Brunauer, Emmett, and Tell or BET method) on isolated platelet samples.

Electrical conductivity seems to be the primary focus of property characterization efforts in these studies, which all confirmed that only a small amount of NGPs or nanoscaled graphite oxide platelets was required to achieve the conductive path percolation for enhanced electrical conductivity of a polymer, which by itself was normally an electrical insulator. The threshold proportions (typically <0.5% in PMMA, <1% in nylon, and <1–2.5% in PS) for percolation were found to be comparable to those in CNT-filled composites.

Recent developments in the preparation of NGPs and NGP nanocomposites

NGPs: recent attempts for the preparation of single-sheet graphene

In 2004, Novoselov and co-workers [1, 2] prepared single-sheet graphene by removing graphene from a graphite sample one sheet at a time using a "Scotch-tape" method. Although this method is not amenable to large-scale production of NGPs, their work did spur globally increasing interest in nanographene materials, mostly motivated by the thoughts that graphene could be useful for developing novel electronic devices [10–18].

Small-scale production of ultra-thin graphene sheets on a substrate can be obtained by thermal decomposition-based epitaxial growth [14] and a laser desorption-ionization technique [79]. However, more promising techniques for mass-producing NGPs are likely those that involve chemical or thermal exfoliation of intercalated graphite or oxidized graphite.

For instance, Chen et al. [73] exposed GO to a temperature of 1,050 °C for 15 s to obtain exfoliated graphite, which was then subjected to ultrasonic irradiation in a mixture solution of water and alcohol. Li et al. [9] followed a similar approach. Jang et al. [80] thermally exfoliated GIC to produce exfoliated graphite (Fig. 4) and subjected exfoliated graphite to mechanical shearing treatments, such as ball milling, to obtain NGPs, which were mostly single- to five-layer structures (Fig. 5). The specific surface area of

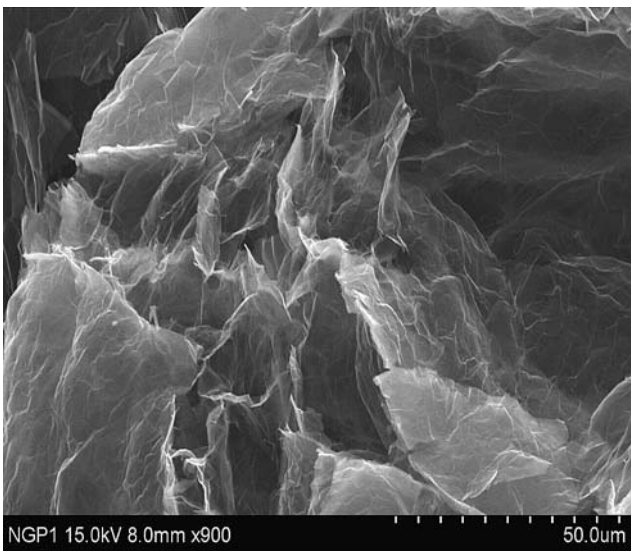

Fig. 4 A SEM image of exfoliated graphite (after sulfuric acid–nitric acid intercalation and thermal shock exposure at 1,050 °C). Exfoliated graphite is characterized by having graphene sheets remaining somewhat interconnected with one another

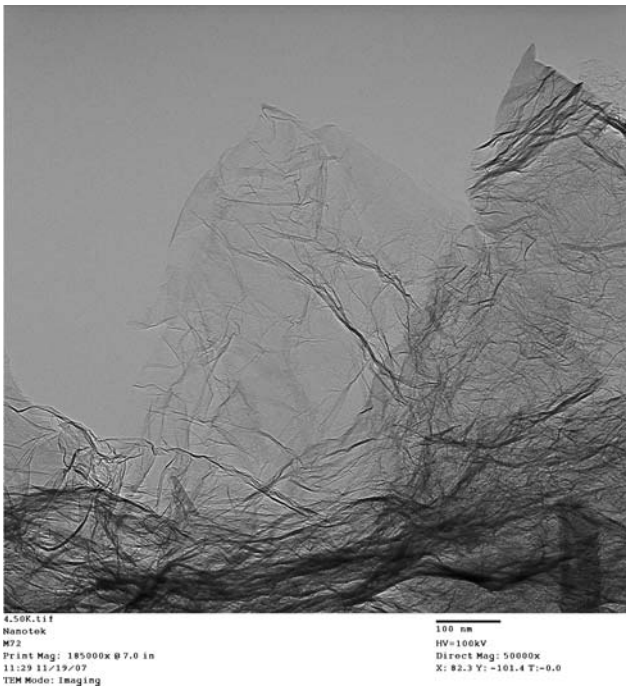

Fig. 5 TEM image of NGPs after ball milling of exfoliated graphite (which was obtained from sulfuric acid–nitric acid intercalation and thermal shock exposure at 1,050 °C). Several graphene sheets collapsed to overlay one another after dispersion in acetone and then cetone removal during the TEM sample preparation procedure

the samples prepared in this method was found to be typically in the range of 300–1,300 m^2/g, as measured by the BET method. Thermal exfoliation as a way of producing nanostructured graphite was also attempted by Petrik [81]. Thermal exfoliation of intercalated graphite was conducted by Drzal et al. [82] using microwaves as a heat source.

Aksay and co-workers [7–9] also used thermal exfoliation of GO to obtain exfoliated graphite oxide platelets, which were found to contain a high proportion of single-layer graphene sheets, based on the BET method with nitrogen gas adsorption in the dry state and in an ethanol suspension with methylene blue dye as a probe. McAllister et al. [6] provided a good model to explain the exfoliation mechanisms and kinetics of GO.

Mack, Viculis, and co-workers [83, 84] developed a low-temperature process that involved intercalating graphite with potassium melt and contacting the resulting K-intercalated graphite with alcohol, producing violently exfoliated graphite containing many ultra-thin NGPs. The process must be carefully conducted in a vacuum or an extremely dry glove box environment since pure alkali metals, such as potassium and sodium, are extremely sensitive to moisture and pose an explosion danger. It is questionable if this process is easily amenable to the mass production of nanoscaled platelets. One major advantage of this process is the notion that it produces non-oxidized graphene sheets since no acid/oxidizer intercalation or a high temperature is involved. Mack et al. [85] also investigated electro-spinning of NGP-containing polymers as a means of creating nanocomposites.

Stankovich et al. [23] followed the approaches of Hirata et al. [34–36] to produce and disperse graphite oxide sheets in water to obtain stable colloidal dispersions. The graphite oxide dispersion was then reduced with hydrazine, a procedure previously used by Liu and Gong earlier [39], but in the presence of poly (sodium 4-styrenesulfonate). This process led to the formation of a stable aqueous dispersion of polymer-coated graphene platelets. Stankovich et al. [24] further developed a method to produce less hydrophilic GO platelets using an isocyanate treatment. However, unless stabilized by selected polymers, the chemically modified graphene sheets obtained through these methods tend to precipitate as irreversible agglomerates due to their hydrophobic nature. The resulting agglomerates became insoluble in water and organic solvents. Li et al. [86] overcame this issue by using ammonium to adjust the pH value of a dispersion of chemically modified graphene sheets in water, which served to maximize the charge density on the resulting graphene sheets. The resulting electrostatic forces acted to stabilize the aqueous suspension.

Some of the earlier work on graphene preparation was recently reviewed by Geim and Novoselov [87].

NGP nanocomposites

Chemical compatibility between a filler and a matrix is a critical factor to consider in the preparation of a composite material. This is also true of a nanocomposite consisting of a polymer and a nanofiller, such as CNT or NGP. Graphite oxide and partially reduced GO platelets are known to have very active surface or edge functional groups, such as carboxyl, carbonyl, epoxide, and hydroxyl. These groups enable GO platelets to readily disperse in water or a polar solvent to form stable colloidal suspensions and, hence, can be readily mixed with a water-soluble polymer, such as poly (ethylene oxide) [60–65] and poly (vinyl alcohol) [50–52]. GO platelets are expected to be miscible with polar chains or polymers with a polar side group [21]. Furthermore, by chemically modifying the functional groups one could tailor GO platelets' compatibility with a desired polymer [e.g., 88]. Graphite oxide can also act as an oxidizing reagent for the in situ polymerization of aromatic dithiols, with the resulting reduced GO well dispersed in the polymer [89].

Stankovich et al. [25] proposed a general approach for the preparation of graphene–polymer composites via complete exfoliation of GO and dispersion of individual GO sheets within polymer hosts. The GO sheets are then

chemically reduced to partially restore back to graphite. As an example, a polystyrene–graphene composite formed with this method exhibits an electrical conductivity percolation threshold of 0.1% by volume at room temperature. This is by far the lowest reported threshold value for any carbon-based composite except for those involving carbon nanotubes. This chemical approach of tuning the graphene sheet properties provides a versatile platform for designing new, graphene-based nanomaterials.

Both CNTs and CNFs, being long and thin, can easily get entangled with one another or form a "bird's nest" structure. Hence, the loading of these conductive nanofillers increases the viscosity of the matrix resin to a level that is not conducive to composite processing. This is not the case for the NGP-resin systems wherein the two-dimensional platelets can slide over one another, leading to low resistance-to-shear flow, even at a relatively high NGP proportion. This feature would enable easier application of structural adhesives and more convenient melt processing of polymer nanocomposites containing a high NGP loading.

Fundamentals of NGP production

Most of the processes used for making separated graphene platelets begin with intercalating lamellar graphite particles with an intercalant, followed by expanding the intercalant to exfoliate the flake particles through thermal decomposition, electrostatic repulsion, or chemical reactions.

These processes have yet to be optimized to enable the most cost-effective mass production of NGPs with desired morphology, dimensions, and surface or edge functionalities. Specifically, there are fundamental questions that need to be answered before the NGP technology can be fully commercialized for a range of industrial applications: (1) What are the dominant mechanisms and kinetics of gas phase intercalation of graphite? (2) What are the dominant mechanisms and kinetic factors of gas or electrostatic exfoliation of graphite and full separation of graphene platelets? (3) How low a temperature can one use to exfoliate graphite for the preparation of NGPs. (4) Under what conditions can one freely produce single graphene sheets of desired dimensions. Models for thermodynamics, kinetics, and mechanisms of intercalation and exfoliation of graphite must be established to guide experimental research.

Phenomenological model for graphite exfoliation

To gain an in-depth understanding of the exfoliation of graphite layers, we may first consider the "gas bubble model" (GBM) originally developed by Martin and Brocklehurst [90] for explaining the large-scale thermal expansion behavior of bromine-intercalated pyrolytic graphite compounds. The original model assumes that the bromine exists in the form of gaseous bubbles residing in the inter-layer spacing (e.g., Fig. 6). The bubbles are assumed to be penny-shaped, each with its axis parallel to the crystal c-axis and having a thickness c_s equal to the saturation inter-layer spacing (0.705 nm for bromine-intercalated graphite) and with a radius r perpendicular to the c-axis, depending on the temperature and amount of bromine gas in the bubble, the externally applied stress S, and the lattice energy resisting bubble expansion. The magnitude of S may be related to the notion that the expansion of a crystallite in a polycrystalline graphite particle is constrained by its surrounding crystallites. The lattice energy resisting bubble expansion is related to the van der Waals forces that hold individual graphene planes together in the c-axis direction.

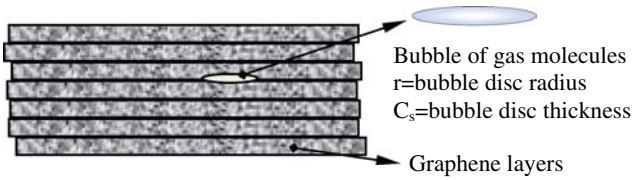

Fig. 6 A proposed gas bubble model used to estimate the negative pressure (stress) required to grow a Griffith crack (delaminating inter-graphene layer)

Consider a graphite crystal of volume V_0 containing N disc-shaped bubbles of radius r. Each bubble may be treated as a Griffith's crack. Without considering plastic deformation, the crack will spread under a tensile stress σ parallel to the c-axis when

$$\sigma = \left[\pi\gamma\mu/2\left(1-\nu^2\right)r\right]^{1/2} \tag{1}$$

where γ is the effective graphite surface energy per unit area of the bubble, ν the Poisson's ratio of graphite, and μ the the shear modulus of the graphite crystal. The values of these physical constants for graphite are available in the literature [90]: $\gamma = 120$ erg/cm^2, $\nu = 0.3$, and $\mu = 3 \times 10^{10}$ dynes/cm^2, leading to a minimum breakaway pressure of approximately 1.6 MPa. The threshold gas pressure P for the bubble to begin to spread (i.e., reaching the critical crack size) may be expressed as

$$P \geq \sigma + S \tag{2}$$

the gas bubble may come from vaporization of pre-existing intercalant molecules (e.g., bromine) or molecules generated by heat-induced chemical decomposition (e.g., SO_2 from sulfate group in sulfuric acid-intercalated graphite). The term S is related to the resistance of neighboring graphite crystallites against the expansion of a crystallite of interest. For simplicity, the gas in the bubble may be assumed to obey the ideal gas law

$$P = nkT/\left(\pi r^2 c_s\right) \tag{3}$$

where n = number of gas molecules or atoms in the bubble, T = absolute temperature, and k = Boltzmann's constant, although a more accurate estimation may be obtained from an equation-of-state formulation. Combining Eqs. 1–3, we obtain the threshold condition for the initiation of an irreversible expansion of graphene layers

$$P = nkT/\left(\pi r^2 c_s\right) \geq \left[\pi\gamma\mu/2\left(1-\nu^2\right)r\right]^{1/2} + S. \tag{4}$$

In a study of bromine-intercalated graphite, Anderson and Chung [91, 92] proposed that buckling of the crack walls (rather than the brittle Griffith mode) was responsible for the exfoliation of graphite by bromine vapor. This buckling mode was presumed to occur when large bending moments existed at the crack tip. Experimentally, the exfoliation stress for a bromine-intercalated graphite sample was found to be approximately 1.3 MPa at 200 °C. However, Anderson and Chung did not offer an estimate on the required bending moment, nor did they provide direct evidence to support their hypothesis. A more comprehensive model will have to account for large-scale deformations or expansions in addition to the initiation of an unstable growth. Prior to the establishment of such a model, Eq. 4 provides a working guideline for designing proper gas-intercalated graphite composition and subsequent exfoliation conditions.

Mechanistic model for graphite exfoliation

In a study of heat-induced exfoliation of heavily oxidized graphite (GO), McAllister et al. [6–8] concluded that CO_2 induced by the decomposition of oxygen-containing groups in the GO provided the gas pressure that drove the exfoliation process. To calculate the pressure required to exfoliate GO, McAllister et al. considered GO as a multi-layer system and applied Lifshitz's formulation of van der Waals forces to calculate the binding energy between two adjacent layers [6, 93]. Specifically, in this model, GO was treated as a multi-layer system composed of hydrocarbon sheets. The exfoliation process was initiated at a particular weak inter-layer spacing susceptible to rupture due to gas pressure. The pressure needed to overcome van der Waals binding was then given by:

$$P = (\partial G/\partial l) = A_{\text{Ham}}/\left(6\pi l^3\right) \tag{5}$$

where G was the interaction free energy per unit area between two semi-infinite slabs, A_{Ham} was the Hamaker coefficient ($A_{\text{Ham}} = 2.37 \times 10^{-21}$ J), and l was the inter-layer distance. Because the van der Waals force is inversely proportional to l^3 and the pressure generated from evolved gases is inversely proportional to l, once the exfoliation process in GO is initiated, the multi-layer binding is ruptured at an accelerating pace. By numerically evaluating the Hamaker constant, the pressure required to separate two GO sheets was estimated to be 2.5 MPa [6]. In this treatment, GO was regarded as a multi-layer system composed of insulating sheets. If the layers are treated as graphene, the required pressure was increased to 7.2 MPa.

To estimate the maximum pressures that could be generated by the evolution of CO_2 from their heavily oxidized GO, McAllister et al. [6] proceeded to obtain a CO_2 density of 9,300 mol/m^3. The force exerted on the GO surface was then calculated from the molecular motion approach. The calculated pressure ranged from 40 MPa at 200 °C (the decomposition temperature of GO) to 130 MPa at 1,000 °C. With the dimensions of the gap in the system studied being close to the atomic scale, the actual pressure may be best calculated using the kinetic theory of gases. In this case, the calculated pressures would be in excess of 200 and 600 MPa at 200 and 1,000 °C, respectively [6]. The estimated pressures generated during exfoliation were one to two orders of magnitude greater than the van der Waals forces binding the GO sheets together.

Kinetic aspects of exfoliation

The above pressure calculations were performed assuming that the gas could not escape the inter-layer region of GO before the expansion occurred. However, the van der Waals forces may be sufficient to avoid exfoliation if gas evolution and expansion occurs slowly enough that lateral diffusion can relieve the generated pressure. The diffusion time scale calculated from Knudsen diffusion was on the order of 10^{-4} s, but decreasing with increasing temperature [6].

To determine the critical temperature at which the reaction time scale was shorter than the diffusion time scale, McAllister et al. [6] monitored the isothermal decomposition of GO at varying temperatures using TGA. The experimental data were found to follow Arrhenius behavior [6]. The decomposition data followed second-order kinetics with respect to oxygen content. The reaction time scale was estimated from $1/k'(1-\alpha)$, where α is the fractional conversion of oxygen chemically bound to the GO, and k' is the reaction rate constant. The total mass loss of GO upon heating could be determined by TGA, and the fractional conversion was the mass evolved relative to the total mass loss. For this scaling analysis, the initial concentration of functional groups was used, where the fractional conversion was zero. With the kinetic parameters thus determined, the reaction time scale and the diffusion time scale were plotted as shown in Fig. 7. One can see that at a temperature of 550 °C or higher, the reaction time scale is shorter than the diffusion time scale.

Thus far, no analytical model has been proposed to explain the exfoliation of graphite or graphite oxide due to electrostatic repulsion.

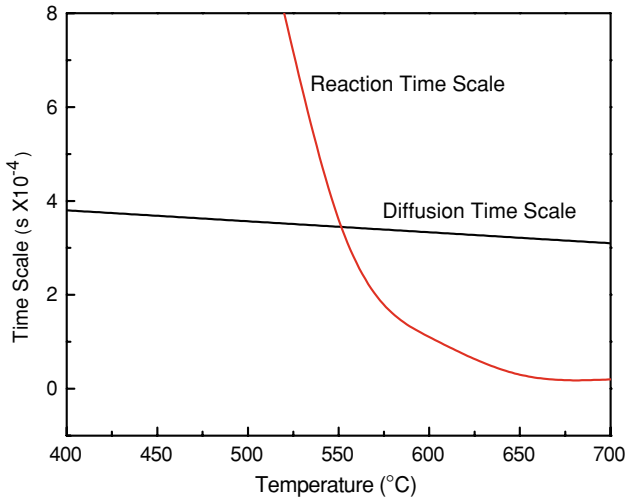

Fig. 7 Competition between the gas escape rate and gas production rate [6]

Potential applications of NGPs and NGP nanocomposites

For scientific and engineering applications, anticipated features and benefits of NGP-based materials include the following:

(1) Nanographene exhibits many peculiar electronic, optic, magnetic, and chemical properties (and many more that may have yet to be uncovered) that enable many potential device applications [1, 2, 10–18]. Potential application of NGPs in field effect transistors was recently discussed by Gomez-Navarro et al. [94] and by Gilje et al. [95].

(2) In addition to much lower costs (compared to carbon nanotubes, CNTs), another major advantage of graphene-based nanocomposites is their capability of forming a thin film, paper [96], or coating for electromagnetic interference (EMI) shielding and electrostatic charge dissipation (ESD) applications when the NGP loading exceeds the percolation threshold so that platelets form a network of electron transport paths.

(3) Due to the ultra-high thermal conductivity of NGPs (four times more thermally conductive, yet four times lower in density compared to copper), a nanocomposite thin film, paper, or coating can be used as a thermal management layer in a densely packed microelectronic device.

(4) When a high loading of NGPs (5–75 wt%) is incorporated into a polymer or carbon matrix, the resulting nanocomposite possesses an exceptionally high electrical conductivity for fuel cell bipolar plate applications [97, 98].

(5) NGP nanocomposites have a good combination of mechanical stiffness, strength, micro-cracking resistance, electrical and thermal conductivities, and barrier performance at a minimal filler concentration. The mechanical properties are reasons why NGPs have been used in making golf balls [99] and micro-composite containers for hydrogen storage [100]. The NGP nanocomposites are truly multifunctional.

(6) NGP composites (in the form of a conductive paper/film/coating, structural adhesive, etc.) can be an integral part of lightning strike protection strategies for aircraft, telecommunication towers, and wind turbine blades.

(7) NGPs can be a component material for lithium ion battery electrodes. For instance, self-assembled graphite oxide nanoplatelets and polyelectrolytes can be a cathode material that provides an exceptionally high specific capacity [66].

(8) Ultra-thin graphene films, being optically transparent and electrically conductive are a potential alternative to the metal oxide window electrodes for solid-state, dye-sensitized solar cells [101]. Graphene–silica composite thin films [102] are good transparent conductors that have many potential applications, including solar reflecting windshields, self-cleaning windows, electrostatic charge-dissipating coatings, and sensor devices.

(9) For supercapacitor electrode applications, NGP-based materials possess the following desirable features: (a) The dimensions of platelets can be tailored to obtain NGPs with a thickness as low as $\sim$0.34 nm and length (width) range of $\sim$100 nm–10 μm, yielding a specific area of up to 2,600 m^2/gm (Fig. 1); and (b) the surfaces of NGPs can be functionalized, particularly via surface grafting or polymerization, to achieve pseudo-capacitance induced by redox-like charge transfer.

Future research directions

In summary, current methods of producing NGPs have several serious drawbacks that must be overcome. These issues present good challenges and opportunities for future research:

(1) One common feature of these methods is the utilization of liquid or solution-based chemicals to intercalate graphite particles. These chemicals often include strong acids (e.g., sulfuric or nitric acids) or other undesirable species that can reside in the material.

(2) When undesirable chemicals are used, a tedious washing step is required, which produces contaminated waste water that requires costly disposal steps.

(3) Acid intercalation treatments also result in oxidation of graphite, which has much lower electrical and thermal conductivities compared with unoxidized graphite.
(4) The approach proposed by Mack et al. [83, 84] involves intercalating graphite with potassium melt (hence, no oxidation issue), which must be carefully conducted in a vacuum or in an extremely dry glove box environment since pure alkali metals like potassium and sodium are extremely sensitive to moisture and pose an explosion danger. It is clear that this process is not amenable to mass production of nanoscaled platelets.
(5) Additional models for graphite intercalation and exfoliation need to be developed for guiding future research on the fabrication of nanographene materials.
(6) The observations that the threshold NGP proportion for electrical conductivity path percolation varies from one polymer to another and from one NGP geometry (e.g., length-to-thickness aspect ratio) to another remain to be satisfactorily explained.
(7) Mass production methods of preparing large-area, single graphene sheets are needed before practical graphene-based nanoelectronics can be realized.

Conclusions

Processing techniques for nanographene platelets and their nanocomposites have been reviewed. More significant or promising processes published in both open literature and patent documents were included in the discussion. The fundamental principles that could guide the design and development of future graphene production processes were briefly introduced. Also briefly summarized were potential applications of this rapidly emerging class of nanomaterials and some of the technical issues that must be addressed before broad applications of these materials can be realized.

References

1. Novoselov KS, Geim AK, Morozov SV et al (2004) Science 306:666. doi:10.1126/science.1102896
2. Novoselov KS, Jiang D, Schedin F et al (2005) Proc Natl Acad Sci USA 102:10451. doi:10.1073/pnas.0502848102
3. Jang BZ, Huang WC (2006) US Patent 7,071,258, (submitted on 21 Oct 2002 and issued on 4 Jul 2006)
4. Jang BZ (2006) US Patent 11/442,903 (20 Jun 2006); a divisional of 10/274,473 (21 Oct 2002)
5. Schwalm W, Schwalm M, Jang BZ (2004) American Physical Society Montreal, Canada
6. McAllister MJ, Li JL, Adamson DH et al (2007) Chem Mater 19:4396. doi:10.1021/cm0630800
7. Li JL, Kudin KN, McAllister MJ et al (2006) Phys Rev Lett 96:176101. doi:10.1103/PhysRevLett.96.176101
8. Schniepp HC, Li JL, McAllister MJ et al (2006) J Phys Chem B 110:8535. doi:10.1021/jp060936f
9. Li X, Wang X, Zhang L, Lee S et al (2008) Science 319:1229–1. doi:10.1126/science.1150878
10. Novoselov KS, Geim AK, Morozov SV et al (2005) Nature 438:197. doi:10.1038/nature04233
11. Zhang Y, Ando T (2002) Phys Rev Lett B65:245420
12. Zhang Y, Tan YW, Stormer HL et al (2005) Nature 438:201. doi:10.1038/nature04235
13. Zhang Y, Small JP, Amori ME et al (2005) Phys Rev Lett 94:176803. doi:10.1103/PhysRevLett.94.176803
14. Berger C, Song Z, Li T et al (2004) J Phys Chem B 108:19912. doi:10.1021/jp040650f
15. Enoki T, Kobayashi Y (2005) J Mater Chem 15:3999. doi:10.1039/b500274p
16. Heersche HB, Jarillo-Herrero P, Oostinga JB et al (2007) Nat Lett 446:56. doi:10.1038/nature05555
17. Soon YW, Cohen ML, Louie SG (2006) Nat Lett 444:347. doi:10.1038/nature05180
18. Meyer JC, Geim AK, Katsnelson MI et al (2007) Nat Lett 446:60. doi:10.1038/nature05545
19. Wong SC, Sutherland EM, Jang BZ (2004) Proceedings of the 62nd SPE ANTEC, Chicago, IL, 2004
20. Wong SC, Sutherland E, Jang BZ (2004) Proceedings of NSF design and manuf. Grantees and research Conf. Dallas, TX, 2004
21. Fukushima H, Lee SH, Drzal LT (2004) Proceedings of the 62nd SPE ANTEC, Chicago, IL, 2004
22. Yasmin A, Daniel IM (2004) Polymer 45:8211. doi:10.1016/j.polymer.2004.09.054
23. Stankovich S (2006) J Mater Chem 16:155. doi:10.1039/b512799 h
24. Stankovich S, Piner RD, Nguyen ST et al (2006) Carbon 44:3342. doi:10.1016/j.carbon.2006.06.004
25. Stankovich S, Dikin DA, Dommett G et al (2006) Nat Lett 442:282. doi:10.1038/nature04969
26. Bunnell LR Sr (1991) US Patent 987(4):175
27. Bunnell LR Sr (1991) US Patent 019(5):446
28. Bunnell LR Sr (1993) US Patent 186(5):919
29. Zaleski PL, Derwin DJ, Girkant RJ et al (2001) US Patent 287(6):694
30. Mazurkiewicz M (2002) US Patent Application No. 09/951,532; Pub. No. US 2002/0054995 (Published on 9 May 2002)
31. Shioyama H (2001) J Mater Sci Lett 20:499. doi:10.1023/A:1010907928709
32. Horiuchi S, Gotou T, Fujiwara M et al (2004) Appl Phys Lett 84:2403 (paper received on 8 September 2003)
33. Horiuchi S, Gotou T, Fujiwara M et al (2003) Jpn J Appl Phys 42(Part 2):L1073. doi:10.1143/JJAP.42.L1073
34. Hirata M, Horiuchi S (2003) US Patent 596(6):396
35. Hirata M, Gotou T, Ohba M (2005) Carbon 43:503. doi:10.1016/j.carbon.2004.10.009
36. Hirata M, Gotou T, Horiuchi S et al (2004) Carbon 42:2929
37. Hummers WS (1957) US Patent 798(2):878
38. Hummers WS (1958) J Am Chem Soc 80:1339. doi:10.1021/ja01539a017
39. Liu P, Gong K (1999) Carbon 37:706. doi:10.1016/S0008-6223(99)00037-8
40. Dekany I, Kruger-Grasser R, Weiaa A (1998) Colloid Polym Sci 276:570. doi:10.1007/s003960050283
41. Roy HV, Kallinger C, Marsen B et al (1998) J Appl Phys 83:4695. doi:10.1063/1.367257
42. Lu XK, Yu MF, Huang H et al (1999) Nanotechnology 10:269. doi:10.1088/0957-4484/10/3/308

43. Land TA, Michely T, Behm RJ et al (1992) Surf Sci 264:261. doi:10.1016/0039-6028(92)90183-7
44. Nagashima A, Nuka K, Itoh H et al (1993) Surf Sci 291:93. doi:10.1016/0039-6028(93)91480-D
45. van Bommel AJ, Crombeen JE, van Tooren A (1975) Surf Sci 48:463. doi:10.1016/0039-6028(75)90419-7
46. Forbeaux I, Themlin J-M, Debever JM (1998) Phys Rev B 58:16396. doi:10.1103/PhysRevB.58.16396
47. Oshima C, Nagashima A (1997) J Condens Matter 9:1. doi:10.1088/0953-8984/9/1/004
48. Wu Y, Chong C (2003) US Patent Appl. No. 10/124,188 (US Pub. No. 2003/0129305, 10 July 2003)
49. Shioyama H (1997) Carbon 35:1664. doi:10.1016/S0008-6223(97)82797-2
50. Matsuo Y, Tahara K, Sugie Y (1998) Chem Mater 10:2266. doi:10.1021/cm980203a
51. Xu JY, Hu Y, Song L et al (2001) Polym Degrad Stab 73:29. doi:10.1016/S0141-3910(01)00046-5
52. Xu JY (2002) Carbon 40:445. doi:10.1016/S0008-6223(01)00133-6
53. Xu JY, Hu Y, Song L et al (2001) Mater Res Bull 36:1833. doi:10.1016/S0025-5408(01)00662-6
54. Xu JY (2002) Carbon 40:2961. doi:10.1016/S0008-6223(02)00207-5
55. Liu PG, Gong K, Xiao P et al (2002) J Mater Chem 10:933. doi:10.1039/a908179 h
56. Matsuo Y, Sugie Y (1998) Carbon 36:301. doi:10.1016/S0008-6223(98)80120-6
57. Xiao P, Xiao M, Liu PG et al (2000) Carbon 38:626. doi:10.1016/S0008-6223(00)00005-1
58. Hamwi A, Marchand V (1996) J Phys Chem Solids 57:867. doi:10.1016/0022-3697(96)00364-2
59. Lerf A, He HY, Forester M (1998) J Phys Chem B 102:4477. doi:10.1021/jp9731821
60. Matsuo Y, Tahara K, Sugie Y (1996) Carbon 34:672. doi:10.1016/0008-6223(96)85961-6
61. Kotov NA, Dekany I, Fendler JH (1996) Adv Mater 8:637. doi:10.1002/adma.19960080806
62. Matsuo Y, Tahara K, Sugie Y (1997) Carbon 35(1):113. doi:10.1016/S0008-6223(96)00123-6
63. Cassagneau T, Fendler JH (1998) Adv Mater 10(11):877. doi:10.1002/(SICI)1521-4095(199808)10:11<877::AID-ADMA877>3.0.CO;2-1
64. Cassagneau T, Guerin F, Fendler JH (2000) Langmuir 16:7318. doi:10.1021/la000442o
65. Kovtyukhova NI, Ollivier PJ, Martin BR et al (1999) Chem Mater 11:771. doi:10.1021/cm981085u
66. Szabo T, Szeri A, Dekany I (2005) Carbon 43:87. doi:10.1016/j.carbon.2004.08.025
67. Xiao P, Xiao M, Gong KC (2001) Polymer 42:4813. doi:10.1016/S0032-3861(00)00819-3
68. Xiao M, Sun LY, Liu JJ et al (2001) Polymer 43(8):2245. doi:10.1016/S0032-3861(02)00022-8
69. Chen GH, Wu DJ, Weng W et al (2001) J Appl Polym Sci 82:2506. doi:10.1002/app.2101
70. Chen GH (2003) Polymer (Guildf) 44:1781. doi:10.1016/S0032-3861(03)00050-8
71. Chen GH, Wu D, Weng W (2003) Carbon 41:619. doi:10.1016/S0008-6223(02)00409-8
72. Chen GH, Weng W, Wu D et al (2003) Eur Polym J 39:2329. doi:10.1016/j.eurpolymj.2003.08.005
73. Chen GH (2004) Carbon 42:753. doi:10.1016/j.carbon.2003.12.074
74. Zheng W, Wong SC, Sue HJ (2002) Polymer 73:6767. doi:10.1016/S0032-3861(02)00599-2
75. Zheng W, Wong SC (2003) Compos Sci Technol 63:225. doi:10.1016/S0266-3538(02)00201-4
76. Pan YX, Yu Z, Ou Y et al (2000) J Polym Sci Part B. Polym Phys 38:1626. doi:10.1002/(SICI)1099-0488(20000615)38:12,<1626::AID-POLB80>3.0.CO;2-R
77. Shen JW, Chen XM, Huang WY (2003) J Appl Polym Sci 88:1864. doi:10.1002/app.11892
78. Du XS, Xiao M, Meng YZ et al (2004) Synth Met 143:129. doi:10.1016/j.synthmet.2003.10.023
79. Udy JD (2006) US Patent Application No. 11/243,285 (Oct. 4, 2005); Pub No. 2006/0269740 (30 Nov 2006)
80. Jang BZ, Wong SC, Bai Y (2005) US Patent Appl. No. 10/858,814 (3 June 2004); Pub. No. US 2005/0271574 (Pub. 8 Dec 2005)
81. Petrik VI (2006) US Patent Appl. No. 11/007,614 (7 Dec 2004); Publ No. US 2006/0121279 (Pub. 8 June 2006)
82. Drzal LT, Fukushima H (2006) US Patent Appl. No. 11/363,336 (27 Feb 2006); 11/361,255 (Feb. 24, 2006); 10/659,577 (10 Sept 2003)
83. Mack JJ, Viculis LM, Kaner RB et al (2005) US Patent 872(6):330
84. Viculis LM, Mack JJ, Kaner RB (2003) Science 299:1361. doi:10.1126/science.1078842
85. Mack JJ, Viculis LM, Ali A et al (2005) Adv Mater 17:77. doi:10.1002/adma.200400133
86. Li D, Muller MC, Gilje S et al (2008) Nat Nanotechnol 3:101. doi:10.1038/nnano.2007.451
87. Geim AK, Novoselov KS (2007) Nat Mater 6:183. doi:10.1038/nmat1849
88. Li J, Kim JK, Sham ML (2005) Scr Mater 53:235. doi:10.1016/j.scriptamat.2005.03.034
89. Du XS, Xiao M, Meng YZ et al (2005) Carbon 43:195. doi:10.1016/j.carbon.2004.06.036
90. Martin WH, Brocklehurst JE (1964) Carbon 1:133. doi:10.1016/0008-6223(64)90067-3
91. Chung DDL (1987) J Mater Sci 22:4190. doi:10.1007/BF01132008
92. Anderson SH, Chung DDL (1984) Carbon 22(3):253. doi:10.1016/0008-6223(84)90169-6
93. Span R, Wagner WA (1996) J Phys Chem Ref Data 25:1509
94. Gomez-Navarro C, Weitz RT, Bittner AM et al (2007) Nano Lett 7(11):3499. doi:10.1021/nl072090c
95. Gilge S, Han S, Wang M et al (2007) Nano Lett 7(11):3394. doi:10.1021/nl0717715
96. Dikin DA (2007) Nat Lett 448:457. doi:10.1038/nature06016
97. Jang BZ, Zhamu A, Song L (2006) US Patent Application No. 11/324,370 (4 Jan 06)
98. Song L, Guo J, Zhamu A et al (2006) US Patent Application No. 11/328,880 (11 Jan 06)
99. Sullivan MJ, Ladd DA (2006) US Patent 7,156,756 (2 Jan 2007) and No.7,025,696 (11 April 2006)
100. Jang BZ (2007) US Patent 186(7):474
101. Wang X, Zhi L, Mullen K (2008) Nano Lett 8(1):323. doi:10.1021/nl072838r
102. Watcharotone S, Dikin DA, Stankovich S et al (2007) Nano Lett 7(7):1888. doi:10.1021/n1070477+S1530-6984(07)00477-8